

Task Guided Representation Learning using Compositional Models for Zero-shot Domain Adaptation

Shuang Liu,¹ Mete Ozay²

¹ RIKEN Center for AIP

Abstract

Zero-shot domain adaptation (ZDA) methods aim to transfer knowledge about a task learned in a source domain to a target domain, while data from target domain are not available. In this work, we address learning feature representations which are invariant to and shared among different domains considering task characteristics for ZDA. To this end, we propose a method for task-guided ZDA (TG-ZDA) which employs multi-branch deep neural networks to learn feature representations exploiting their domain invariance and shareability properties. The proposed TG-ZDA models can be trained end-to-end without requiring synthetic tasks and data generated from estimated representations of target domains. The proposed TG-ZDA has been examined using benchmark ZDA tasks on image classification datasets. Experimental results show that our proposed TG-ZDA outperforms state-of-the-art ZDA methods for different domains and tasks.

Introduction

In real-world applications, distribution of training data of a machine learning algorithm obtained from source domain \mathcal{D}_{sr} may diverge from that of its test data obtained from target domain \mathcal{D}_t . This problem is called domain shift. Machine learning models trained under domain shift suffer from a significant performance drop. For example, a model trained for detecting vehicles using a dataset collected in sunny days (e.g. from a source domain \mathcal{D}_{sr}) performs well for inference on another dataset of vehicles collected in sunny days (e.g. from the same domain \mathcal{D}_{sr}). However, the trained model may perform poorly on a dataset of vehicles collected in rainy days (e.g. from a target domain \mathcal{D}_t). This problem becomes acute for deep neural networks (DNNs) which require massive amount of data for training.

A solution to this problem is fine-tuning models pre-trained on \mathcal{D}_{sr} with data collected from \mathcal{D}_t . However, this solution demands considerable amount of labeled training data from \mathcal{D}_t , which may not be available in many applications, e.g. medical informatics. To overcome this problem, *Domain adaptation (DA)* methods aim to train a model on a dataset from \mathcal{D}_{sr} , so that the trained model can perform well on a test dataset from \mathcal{D}_t . DA methods which train models using unlabelled data from \mathcal{D}_t are called unsupervised domain adaptation (UDA) methods (Bousmalis et al. 2017; Lee

et al. 2019; Chen et al. 2020). UDA methods require large amount of unlabelled data from \mathcal{D}_t to train models. However, this assumption may not be valid in various real-world applications. For instance, access to \mathcal{D}_t may be limited or \mathcal{D}_t may be updated dynamically as in lifelong learning and autonomous driving. To address this problem for training models without using labels and unlabelled data from \mathcal{D}_t , zero-shot domain adaptation (ZDA) methods were proposed (Peng, Wu, and Ernst 2018; Wang and Jiang 2019).

ZDDA (Kutbi, Peng, and Wu 2021) is a DNN based method proposed for ZDA. ZDDA models are trained in three phases across four modules, therefore, they are inconvenient to be deployed in various applications. CoCoGAN (Wang and Jiang 2021) and its variations (Wang and Jiang 2020; Wang, Cheng, and Jiang 2021) extended CoGAN (Liu and Tuzel 2016) to synthesize samples in missing domains for solving the ZDA problem. However, they cannot guarantee that their proposed GAN learns the real distribution of the missing domains. HGnet (Xia and Ding 2020) aims to learn domain invariant features, but does not incorporate feature shareability among domains and across tasks, which is demonstrated to be beneficial for ZDA.

We address the ZDA problem (Figure 1) employing invariance (Zhao et al. 2019) and shareability (Liang, Hu, and Feng 2020) of hypotheses of feature representations in a compositional framework motivated by the recent advances in DA theory (Creager, Jacobsen, and Zemel 2021; Kamath et al. 2021; Li et al. 2021), and observations in deep learning theory (LeCun, Bengio, and Hinton 2015; Saxe, McClelland, and Ganguli 2019; Bau et al. 2020; Lampinen and McClelland 2020; Sejnowski 2020; Poggio, Banburski, and Liao 2020). Our contributions are summarized as follows:

- We propose a ZDA method called Task-guided Multi-branch Zero-shot Domain Adaptation (TG-ZDA) depicted in Figure 2, which takes advantage of invariance and shareability of learned features by the guidance of auxiliary tasks (Figure 1). In TG-ZDA, we first estimate hypotheses of domain invariant and shareable features. To transfer knowledge among domains governing auxiliary tasks, we learn task-aware hypotheses. Then, we integrate them in composite hypotheses by employing a novel end-to-end trainable DNN, since hierarchical compositional functions can be approximated by DNNs without incurring the curse of dimensionality (Poggio, Banburski, and Liao 2020). TG-ZDA does not

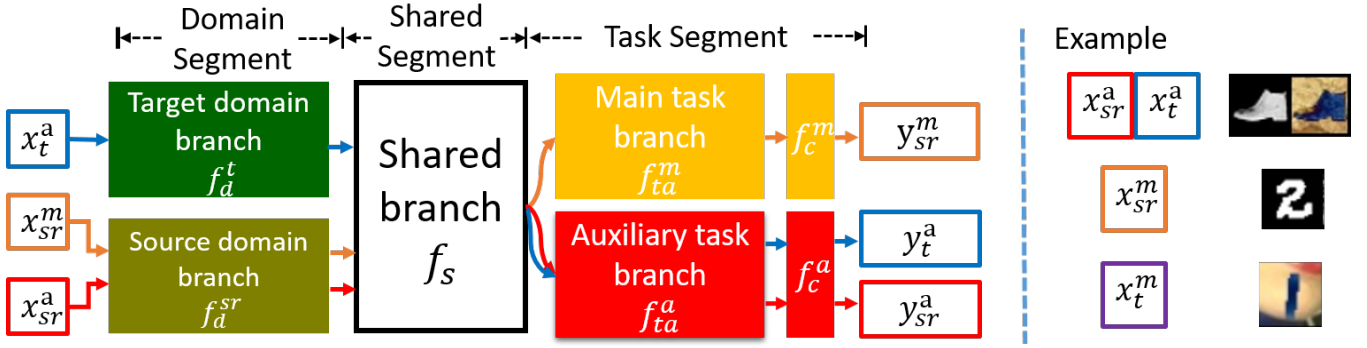


Figure 2: The architecture of the DNN of the TG-ZDA (left) and an input example (right).

$h_c \circ h : x \in \mathcal{X} \mapsto y \in \mathcal{Y}$ of feature representation hypotheses ($h \in \mathcal{H} : x \in \mathcal{X} \mapsto h(x) \in \mathcal{F}$) and classification hypotheses ($h_c \in \mathcal{H} : h(x) \in \mathcal{F} \mapsto y \in \mathcal{Y}$), such that the target risk $\mathbb{E}_{(x,y) \sim \mathcal{D}_t} l(f(x; \mathcal{W}), y)$ measured by a loss function $l(\cdot, \cdot)$ can be minimized by functions $f(\cdot, \mathcal{W})$ approximating $h_c \circ h$ using DNNs. That is, ZDA methods aim first to train a model using \mathcal{X} . Then, the trained model is tested on \mathcal{X}_t^m belonging to the target domain \mathcal{D}_t . To identify structure of $f(\cdot, \mathcal{W})$ by DNNs and optimize its parameters \mathcal{W} , we propose a compositional framework called TG-ZDA depicted in Figure 2 and 3, and described next.

Estimating Composite Hypotheses in TG-ZDA

As shown in Figure 3, data belonging to different domains and associated with different tasks are mapped to a domain independent feature space \mathcal{F} by

$$h_\alpha^\beta \in \mathcal{H}_\alpha^\beta : x_\alpha^\beta \in \mathcal{X}_\alpha^\beta \mapsto h_\alpha^\beta(x_\alpha^\beta) \in \mathcal{F}_\beta, \quad (1)$$

for all $\alpha \in \{sr, t\}, \beta \in \{m, a\}$. Since the dataset \mathcal{X}_t^m belonging to the target domain \mathcal{D}_t is not available in the training phase, estimation of the set of hypotheses \mathcal{H}_t^m is challenging. Domain invariant representations have been employed for solving DA problems (Zhang et al. 2019; Zhao et al. 2019; Johansson, Sontag, and Ranganath 2019; Li et al. 2021) using Invariant Risk Minimization (IRM) (Arjovsky et al. 2020). However, recent works elucidated various limitations of IRM. For instance, IRM does not improve accuracy (Rosenfeld, Ravikumar, and Risteski 2021) or can lead to worse generalization (Kamath et al. 2021) compared to the standard Empirical Risk Minimization (ERM).

More precisely, Rosenfeld et al. show that unless enough domains covering the space of non-invariant features are observed, a domain invariant nonlinear hypothesis can underperform on a new test distribution. Moreover, Kamath et al. show that a sub-optimal hypothesis can be learned using a loss function not being invariant across environments. An attempt to solve this problem is to train models, and selecting domain specific and invariant features by domain specific masks (Chattopadhyay, Balaji, and Hoffman 2020). However, Gulrajani and Lopez-Paz (2020) show that model selection is non-trivial for domain generalization tasks.

Therefore, we address this problem by composition of three different types of hypotheses:

- A *domain dependent* hypothesis function \bar{h} for learning domain specific features.
- A *domain invariant* hypothesis function h^* for learning features shared among multiple domains.
- A *task-aware* hypothesis function \hat{h} for learning feature representations of tasks, and using these representations to guide information transfer among different domains.

Since DNNs can avoid the curse of dimensionality in approximating the class of hierarchically local compositional functions (Poggio, Banburski, and Liao 2020), we approximate hypotheses as follows:

(a) A composite hypothesis $h = \bar{h} \circ h^* \circ \hat{h}$ is approximated by parameterized functions $f(\cdot, \mathcal{W})$ of a DNN, where \mathcal{W} denotes the set of weights of the DNN.

(b) A component of the hypothesis h is approximated by individual functions $f(\cdot, w_{b,k})$, where $w_{b,k} \in \mathcal{W}$ is a weight tensor which will be optimized at the b^{th} branch of the k^{th} segment (i.e. k^{th} group of consecutive layers) of a DNN.

We use (a) and (b) to define a compositional framework called Task-guided Multi-branch Zero-shot Domain Adaptation (TG-ZDA) as illustrated in Figure 2. We use ERM instead of IRM to estimate hypotheses as suggested in the theoretical results proposed in the recent works. We define and control composability of functions among different domains by multiple branches, and segments (i.e. groups of layers) of the DNN used by the TG-ZDA as depicted in Figure 3.

Identifying Hypotheses by Approximating Functions at Branches and Segments of TG-ZDA

TG-ZDA consists of three types of segments, namely (i) domain segment, (ii) shared segment and (iii) task segment. The domain and task segment is domain and task-aware respectively. The shared segment is shared across domains and tasks. The domain segment aims to train hypotheses for using domain specific features and producing domain invariant features. Design of the shared and task segments is inspired by the observations that low-level features are learned at early layers of DNNs, while later layers assemble the learned low-level features into high-level concepts (LeCun, Bengio, and Hinton 2015; Sejnowski 2020). The low-level features shared across tasks are learned by hypotheses at the shared segment. However, characteristics of low-level fea-

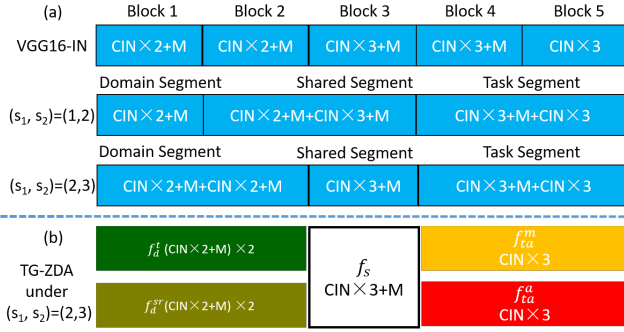


Figure 3: An illustration of different group settings. CIN stands for a convolution layer followed by an instance normalization layer. M stands for a maxpooling layer.

tures assembled in higher layers depend on tasks. To capture these characteristics, a task segment is designed for each task. To this end, each b^{th} branch of the k^{th} segment exploits a parameterized approximation $f(\cdot, w_{b,k} \in \mathcal{W})$ of a composite hypothesis function h as follows:

(i) **Domain Segment:** While designating a domain segment, we consider that hypotheses h_{sr}^d and h_t^d should be estimated successfully for each individual domain using parameterized functions. Hence, functions f_d^{sr} and f_d^t are employed at the source and target domain layer using datasets from domains \mathcal{D}_{sr} and \mathcal{D}_t , respectively. Thereby, *expert* models learned at different branches of TG-ZDA can provide rich representations of individual domains. Therefore, we employ and optimize these functions in different branches of the domain segment without sharing weights.

(ii) **Shared Segment:** A shared segment is designated, taking inspiration from the observation that low-level features are learned at early layers and the low-level features are universal across tasks (Saxe, McClelland, and Ganguli 2019). Features obtained from each domain segment $f_d^\alpha(x_\alpha^\beta)$, $\alpha \in \{sr, t\}$, $\forall \beta \in \{m, a\}$ are fed to the shared segment identifying the function f_s . The function f_s is optimized to learn low-level features shared among the main and auxiliary tasks. A shared segment encodes parameters and serves as an inductive bias to improve generalization.

(iii) **Task Segment:** As Bau et al. (2020) expound, later layers of DNNs assemble low-level detectors to more sophisticated task-aware semantic representations (Lampinen and McClelland 2020). Two functions f_{ta}^m and f_{ta}^a are designed to learn representations for main and auxiliary tasks. They are optimized in different branches of the task segment using output features of f_s of the shared segment.

At last, the features provided by f_{ta}^m and f_{ta}^a are fed to their corresponding classifiers f_c^m and f_c^a , respectively.

In the training phase, the TG-ZDA takes two datasets of samples $\{x_{sr}^m \in \mathcal{X}_{sr}^m\}$ and sample pairs $\{(x_t^a, x_{sr}^a) \in \mathcal{X}_t^a \times \mathcal{X}_{sr}^a\}$ as inputs. Elements in each pair share the same semantic information but from different domains. The TG-ZDA computes class posterior probability of samples belonging to the domain $\alpha \in \{sr, t\}$ for task $\beta \in \{m, a\}$ by $y_\alpha^\beta = f_c^\beta \circ f_{ta}^\beta \circ f_s \circ f_d^\alpha(x_\alpha^\beta)$.

An illustrative example of training a TG-ZDA model:

At the right side of Figure 2, we give an example of inputs for a task to transfer knowledge of models from a domain of grayscale images (\mathcal{D}_{sr}) to a domain of colored images (\mathcal{D}_t). Then, the TG-ZDA is used to transfer the knowledge of models on MNIST (Lecun et al. 1998) with assistance of another task FashionMNIST (Xiao, Rasul, and Vollgraf 2017) (details are given in the next section). Therefore, the main task is defined by classifying samples obtained from MNIST and the auxiliary task is defined by classifying samples belonging to the FashionMNIST and its colored version.

Inference using the trained TG-ZDA model: In the inference phase, TG-ZDA takes x_t^m as the input and computes its class posterior probability by $y_t^m = f_c^m \circ f_{ta}^m \circ f_s \circ f_d^t(x_t^m)$. **Loss Functions:** TG-ZDA models are trained using ERM by minimizing the loss function¹ $L = \gamma L_{cls} + L_D$, where L_{cls} is a classification loss and L_D is a domain discrepancy loss which are balanced by a hyper-parameter $\gamma > 0$.

Classification Loss: The loss function L_{cls} is defined by

$$L_{cls} = \sum_{(\alpha, \beta) \in \{(sr, m), (sr, a)\}} CE(y_\alpha^\beta, \hat{y}_\alpha^\beta), \quad (2)$$

where y_α^β and \hat{y}_α^β is the predicted class posterior probability and its ground truth, respectively for data samples obtained from domain α and task β , and $CE(\cdot)$ denotes the cross-entropy loss. The loss function (2) sums classification losses over different tasks and domains.

Domain Discrepancy Loss: The loss function $L_D = \rho(f_d^t(x_t^a), f_d^{sr}(x_{sr}^a))$ is used to measure domain discrepancy $\rho(\cdot, \cdot)$ of representations. We train TG-ZDA models by minimizing L_D for learning domain invariant feature representations. In the next section, we explore TG-ZDA models trained using ℓ_1 loss, MMD (Borgwardt et al. 2006) and adversarial loss (Tzeng et al. 2017).

Experiments

We first give details of experimental setups such as the datasets and models. Next, TG-ZDA is compared with state-of-the-art methods for multiple ZDA tasks. At last, we examine domain invariance and shareability of features learned using TG-ZDA models. Additional results and implementation details are given in the supplemental material. The code will be provided in the camera-ready version of the paper.

Datasets: Our proposed TG-ZDA is examined on four datasets; MNIST (Lecun et al. 1998), FashionMNIST (Xiao, Rasul, and Vollgraf 2017), NIST (Grother 1970) and EMNIST (Cohen et al. 2017) and their variants, following the experimental settings proposed in (Peng, Wu, and Ernst 2018; Wang and Jiang 2019). The four datasets are denoted by D_M , D_F , D_N and D_E respectively. Their original versions are in gray domain (*G-dom*). The color domain (*C-dom*), the edge domain (*E-dom*) and the negative domain (*N-dom*), are created for each dataset for evaluation.

Network Architecture: We use a VGG16 (Simonyan and Zisserman 2015) with instance normalization (IN) layers denoted by VGG16-IN as the backbone network, and use its

¹Arguments of functions are not shown to simplify notation.

Main task	D_M			D_F			D_E		D_N	
Auxiliary task	D_F	D_N	D_E	D_M	D_N	D_E	D_M	D_F	D_M	D_F
Gray domain to Color domain ($G\text{-dom}, C\text{-dom}$).										
ZDDA	73.2	92.0	94.8	51.6	43.9	65.8	71.2	47.0	34.3	38.7
CoCoGAN	78.1	92.4	95.6	56.8	56.7	71.0	75.0	54.8	41.0	53.8
HGNet	85.3	N/A	95.0	64.5	N/A	71.1	71.3	57.9	N/A	N/A
ALZDA	81.2	93.3	95.0	57.4	58.7	62.0	72.4	58.9	44.6	N/A
DSPZDA	82.9	94.4	95.3	59.1	58.6	63.1	73.6	58.3	46.4	46.5
LTAZDA	81.4	94.8	95.8	62.1	60.0	74.2	79.5	63.3	46.3	49.4
TG-ZDA- ℓ_1	95.5±3.4	96.7±0.2	99.0±0.0	63.4±1.3	49.8±1.3	65.2±1.6	90.9±0.5	87.3±0.3	75.9±0.4	61.7±2.7
TG-ZDA- mmd	97.5±0.2	95.9±0.2	99.1±0.1	45.3±0.3	32.3±1.7	62.2±0.3	90.4±0.9	82.2±2.9	63.0±2.9	40.5±4.4
TG-ZDA- adv	91.9±0.1	95.3±0.0	97.8±0.2	62.2±4.9	49.9±1.2	63.3±2.4	88.6±0.2	71.1±2.4	59.2±2.2	38.1±4.6
Gray domain to Edge domain ($G\text{-dom}, E\text{-dom}$).										
ZDDA	72.5	91.5	93.2	54.1	54.0	65.8	73.6	47.0	42.3	28.4
CoCoGAN	79.6	94.9	95.4	61.5	57.5	71.0	77.9	54.8	48.0	36.3
HGNet	86.5	N/A	96.1	N/A	N/A	N/A	81.1	57.9	N/A	N/A
ALZDA	81.4	93.5	96.3	63.2	58.7	72.4	78.2	58.9	49.9	N/A
DSPZDA	84.7	93.9	95.5	64.8	60.0	73.3	79.2	64.7	50.2	43.3
LTAZDA	81.1	95.0	95.6	66.3	60.7	74.6	78.4	60.6	54.8	51.3
TG-ZDA- ℓ_1	97.0±0.2	96.1±0.5	99.2±0.0	62.8±2.6	47.5±1.3	66.2±2.3	91.0±0.4	73.2±4.1	62.3±1.3	49.0±1.7
TG-ZDA- mmd	96.6±0.6	95.2±0.4	99.1±0.0	53.1±4.2	31.4±2.4	67.6±2.3	89.3±0.3	75.1±2.3	58.7±1.8	32.9±1.2
TG-ZDA- adv	93.8±1.7	95.9±0.4	98.0±0.3	54.6±6.3	48.9±3.3	59.2±1.0	87.5±0.3	70.9±3.3	49.0±2.5	19.4±3.8
Gray domain to Negative domain ($G\text{-dom}, N\text{-dom}$).										
ZDDA	77.9	82.4	90.5	61.4	47.4	65.3	76.2	53.4	37.8	38.7
CoCoGAN	80.3	87.5	93.1	66.0	52.2	66.8	81.1	56.5	45.7	53.8
HGNet	83.7	N/A	95.7	N/A	N/A	71.1	N/A	62.3	N/A	N/A
ALZDA	N/A	N/A	N/A	N/A	N/A	N/A	N/A	N/A	N/A	N/A
DSPZDA	83.6	89.1	94.2	71.1	58.0	70.3	82.1	65.2	49.6	57.4
LTAZDA	81.6	90.4	94.2	68.3	61.5	70.8	81.5	60.3	52.9	56.4
TG-ZDA- ℓ_1	99.2±0.1	99.4±0.0	99.4±0.0	82.4±0.5	83.0±1.3	83.6±0.2	92.3±0.2	91.7±0.2	84.9±0.4	85.0±0.2
TG-ZDA- mmd	99.3±0.0	99.4±0.0	99.3±0.1	82.1±0.9	83.5±0.7	83.2±0.3	92.7±0.1	91.9±0.4	85.6±0.2	85.3±0.2
TG-ZDA- adv	99.1±0.2	99.2±0.1	99.4±0.0	80.4±1.0	77.9±2.7	80.0±0.4	91.6±0.1	90.4±0.2	73.4±2.1	65.8±2.5
Color domain to Gray domain ($C\text{-dom}, G\text{-dom}$).										
ZDDA	67.4	85.7	87.6	55.1	49.2	59.5	39.6	23.7	75.5	52.0
CoCoGAN	73.2	89.6	94.7	61.1	50.7	70.2	47.5	57.7	80.2	67.4
HGNet	78.9	N/A	95.0	65.9	N/A	68.5	N/A	N/A	N/A	N/A
ALZDA	73.4	91.0	93.4	62.4	53.5	71.5	50.6	58.1	83.5	70.9
DSPZDA	76.2	94.6	95.2	63.2	54.3	73.6	84.3	71.5	53.8	61.4
LTAZDA	73.8	93.1	95.0	66.1	54.1	74.3	84.0	77.2	56.4	63.6
TG-ZDA- ℓ_1	98.7±0.2	98.7±0.1	99.0±0.0	74.2±1.7	74.8±1.2	77.4±2.1	85.6±0.7	80.3±0.4	84.0±0.2	82.7±1.0
TG-ZDA- mmd	97.8±0.1	98.4±0.1	98.4±0.2	74.0±3.4	72.1±2.8	70.2±4.8	81.9±1.1	71.0±1.1	83.5±0.5	81.5±0.2
TG-ZDA- adv	96.4±1.3	96.8±0.9	98.3±0.1	70.6±2.0	58.2±6.1	72.5±2.1	80.6±0.8	77.7±2.9	68.9±2.5	67.7±3.9
Negative domain to Gray domain ($N\text{-dom}, G\text{-dom}$).										
ZDDA	78.5	90.7	87.6	56.6	57.1	67.1	34.1	39.5	67.7	45.5
CoCoGAN	80.1	92.8	93.6	63.4	61.0	72.8	47.0	43.9	78.8	58.4
HGNet	87.5	N/A	95.0	64.6	N/A	75.1	78.0	67.9	N/A	N/A
ALZDA	82.6	94.6	95.8	67.0	68.2	77.9	51.1	44.2	79.7	62.2
TG-ZDA- ℓ_1	98.7±0.4	98.3±0.4	99.1±0.0	76.5±0.7	74.7±1.1	74.2±1.0	85.6±0.5	84.0±0.6	85.0±0.5	85.6±0.2
TG-ZDA- mmd	99.0±0.0	98.8±0.0	99.0±0.1	76.3±1.2	75.7±0.4	75.2±1.6	84.9±1.4	84.2±0.3	85.7±0.2	85.4±0.2
TG-ZDA- adv	98.6±0.0	97.3±0.3	99.0±0.1	76.0±0.8	60.0±3.0	75.5±1.5	85.4±1.8	82.8±0.9	73.1±1.7	69.3±2.2

Table 1: Comparison of accuracy (%) of methods. N/A indicates that accuracy is not reported by the corresponding method (red and blue indicates the best and the second best accuracy.). Since the accuracy values of DSPZDA and LTAZDA are not reported in the corresponding papers for ($N\text{-dom}, G\text{-dom}$), they are not shown in the table.

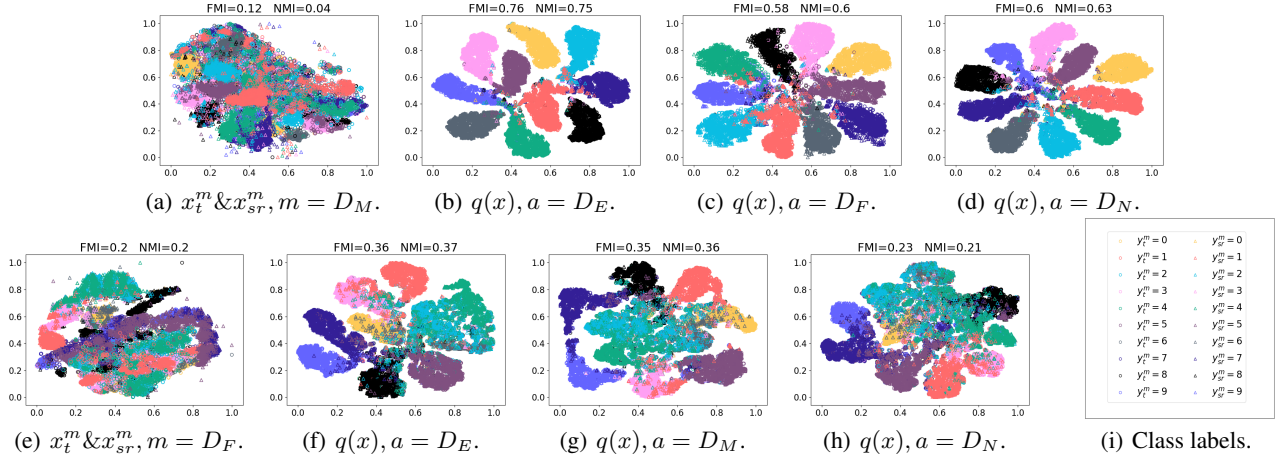


Figure 4: Visualization of distribution of representations using t-SNE when the domain pair is $(G\text{-dom}, C\text{-dom})$. The figures in the first row show features learned when the main task is D_M while the auxiliary task is (b) D_E , (c) D_F and (d) D_N . Similarly, the second row shows figures when the main task is D_F while the auxiliary task is (f) D_E , (g) D_M and (h) D_N . Figures (a) and (e) show distributions of input data x_t^m . Classes of x_t^m are indicated by different colors. Figures (b)-(d) and (f)-(h) show distributions of features computed by $q(x)$ for the corresponding auxiliary tasks, where $q \triangleq f_{ta}^m \circ f_s \circ f_d^\alpha$, $\alpha \in \{s, t\}$, and x denotes either x_t^m or x_{sr}^m . Triangle and circle markers indicate features belonging to the source and target domains.

different partitions as the segments of the TG-ZDA network. Huang and Belongie (2017) showed that the mean and variance of features encode style information of input images. Since style information is highly domain dependent, we consider that IN can be used to extract domain invariant features by statistically normalizing features, helping to disentangle category specific (semantic) and domain specific features.

Design of segments of TG-ZDA: The VGG16-IN consists of five blocks, which are split into three groups by two hyperparameters s_1 and s_2 . The setting $(s_1, s_2) = (1, 2)$ indicates that the VGG-IN is separated into three segments at the first and second maxpooling layer. Each group is used as a segment of the TG-ZDA network. The second and third row of Figure 3-(a) shows an illustration of the three segments obtained for $(s_1, s_2) = (1, 2)$ and $(s_1, s_2) = (2, 3)$. The ReLU is omitted in the figure. The bottom row of Figure 3 shows the architecture for $(s_1, s_2) = (2, 3)$, which is the default setting used in the experiments. All classifiers f_c^β , $\beta \in \{m, a\}$ consist of three fully connected layers.

Comparison with State-of-the-art

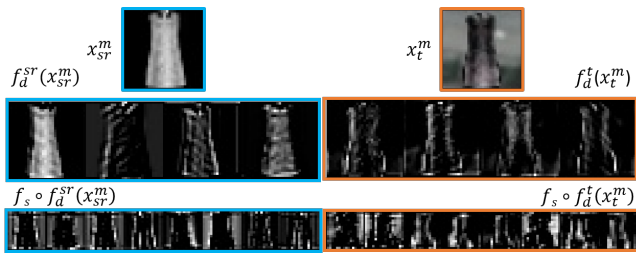
Akin to (Wang and Jiang 2019), we evaluate TG-ZDA for five pairs of source and target domains. $G\text{-dom}$ is set as the source domain in three of them. They are $(G\text{-dom}, C\text{-dom})$, $(G\text{-dom}, E\text{-dom})$, and $(G\text{-dom}, N\text{-dom})$. The other two pairs take $G\text{-dom}$ as the target domain, where the domain pairs are $(C\text{-dom}, G\text{-dom})$ and $(N\text{-dom}, G\text{-dom})$. For each domain pair, we evaluate TG-ZDA on four different tasks corresponding to the four datasets given in the previous section. Each task consists of a main and an auxiliary task. For instance, when a given task is domain adaptation from $G\text{-dom}$ to $C\text{-dom}$ on the MNIST dataset, the Fashion-MNIST can be used to assist TG-ZDA to perform the task. In this case, the main task classifies MNIST digits ($G\text{-dom}$), while the auxiliary task classifies FashionMNIST clothes be-

longing to $G\text{-dom}$ and $C\text{-dom}$. (D_N, D_E) and (D_E, D_N) are not viewed as valid (*main task, auxiliary task*) pairs in our experiments, since they both contain images of letters. We compare TG-ZDA, optimized by ℓ_1 loss, MMD loss (Borgwardt et al. 2006) and adversarial loss (Tzeng et al. 2017) respectively, with six state-of-the-art methods, ZDDA (Peng, Wu, and Ernst 2018; Kutbi, Peng, and Wu 2021), CoCoGAN (Wang and Jiang 2019), ALZDA (Wang and Jiang 2020), LATZDA (Wang and Jiang 2021), HGNet (Xia and Ding 2020) and DSPZDA (Wang, Cheng, and Jiang 2021). TG-ZDA models trained by ℓ_1 , MMD and adversarial loss is denoted by TG-ZDA- ℓ_1 , TG-ZDA-*mmd* and TG-ZDA-*adv*.

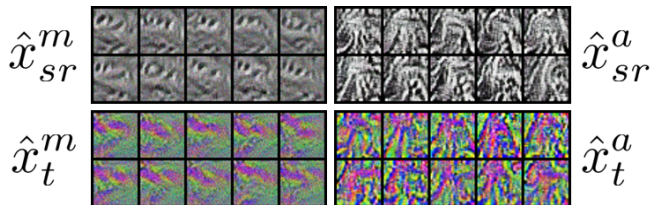
Table 1 provides mean (\pm standard deviation) classification accuracy over three random trials. In the analyses, TG-ZDA achieved top two accuracy in 44 tasks and top one accuracy in 42 tasks out of 50 tasks. Ablation study of loss functions shows that TG-ZDA- ℓ_1 obtained the top-two-accuracy in 44 tasks, and TG-ZDA-*mmd* achieved top-two-accuracy in 37 tasks. We conjecture that the superiority of TG-ZDA- ℓ_1 and TG-ZDA-*mmd* over TG-ZDA-*adv* is due primarily to the fact that TG-ZDA- ℓ_1 and TG-ZDA-*mmd* can learn intermediate domain invariant feature representation by estimating hypotheses at both the source and target branch simultaneously, while TG-ZDA-*adv* matches distribution of features learned at the target domain branch to that of the source domain branch. Even though TG-ZDA-*adv* performs the worst among three TG-ZDA variants, it still outperforms the state-of-the-art methods by a large margin in 34 tasks, demonstrating effectiveness of TG-ZDA.

Analyses of Learned Feature Representations

Feature separability: We visualize representations learned using TG-ZDA with t-SNE (van der Maaten and Hinton 2008) and elucidate their effectiveness. Figure 4 shows results for the domain pair $(G\text{-dom}, C\text{-dom})$ as the



(a) Domain invariant features.



(b) Shareability of features among domains.

Figure 5: (a) Domain invariant features learned by TG-ZDA when the main task is D_F , assisted by D_M . (b) Visualization of features \hat{x}_{sr}^m , \hat{x}_t^m , \hat{x}_{sr}^a and \hat{x}_t^a shared among domains.

main task is D_M and D_F . Figure 4(a) and 4(e) depict distributions of x_t^m from unseen target domain, where its main task is D_M and D_F , respectively. The results show that the samples of x_t^m are not well separable among classes. In contrast, class separability improves in the feature space provided by $q \triangleq f_{ta}^m \circ f_s \circ f_d^\alpha$, $\alpha \in \{sr, t\}$. They are indicated by circle markers in Figure 4(b)-4(d) and 4(f)-4(h) which demonstrate that the segments of TG-ZDA improve separability of x_t^m . However, the results do not indicate that the features of x_t^m can be classified well by f_c^m since f_c^m is trained using x_{sr}^m . If features of x_{sr}^m and x_t^m are well discriminated, then the features of x_t^m can be classified well by f_c^m trained using x_{sr}^m . Triangle markers in Figure 4(b)-4(d) and 4(f)-4(h) demonstrate this property. Triangle and circle markers indicate representations of x_{sr}^m and x_t^m , respectively. Colors of the markers differ by class id. We observe that representations of x_{sr}^m and x_t^m belonging to the same class are well-clustered, demonstrating *good* feature separability among classes.

Alignment of features among domains: We analyze alignment of learned features by first clustering features belonging to the source and target domain using k-means (Lloyd 1982). Then, we compute Fowlkes-Mallows index (FMI) (Fowlkes and Mallows 1983) and normalized mutual information (NMI) (Müller and Guido 2016) for clusters belonging to the source and target domain. $FMI \in [0, 1]$ measures alignment of features between target and source domain considering their class labels, and higher FMI values indicate better alignment. $NMI \in [0, 1]$ measures statistical correlation among clusters of features obtained from different domains, and higher values indicate better correlation.

In Figure 4, features obtained using composite hypotheses provide higher FMI and NMI values. This result shows that feature alignment among different domains is improved by task guided training of compositional hypotheses of rep-

resentations. More precisely, FMI and NMI computed using x_t^m and x_{sr}^m is 0.12 and 0.04 respectively, revealing a bad alignment in Figure 4(a) and 4(e). They increase to 0.76 and 0.75, respectively, indicating a *good* alignment, after mapping x_t^m and x_{sr}^m to feature spaces by $q(x)$. Moreover, the results show that a better cluster and feature alignment results in better classification by comparing Figure 4(b) and 4(f), and their corresponding accuracy in Table 1.

Domain invariance and feature shareability: We visualize feature maps learned using TG-ZDA by optimizing x_α^β to examine the learned domain invariants and benefits of feature shareability among domains. In the analyses, we used (G -dom, C -dom) as the ($source$, $target$) pair. We first depict outputs of the domain and shared segments in Figure 5(a), when the main and auxiliary task is classifying samples from FashionMNIST and MNIST, respectively. The feature maps depict the learned task-aware semantic information. Next, we explore the benefits of learning features shared among tasks and domains using TG-ZDA by visualizing x_α^β which maximize the output y_α^β , $\alpha \in \{sr, t\}$, $\beta \in \{m, a\}$. Through optimization, it searches for inputs \hat{x}_α^β that make neurons of the last layer fire with largest values. To explore shareability properties, we visualize $\hat{x}_{\alpha=t}^{\beta=m}$ and $\hat{x}_{\alpha=sr}^{\beta=a}$, since neither of their corresponding hypotheses have access to x_α^β . We observe that \hat{x}_α^β is in the domain α and contains patterns from the task β . This result suggests that ZDA is established through shareability of features among domains and tasks.

In addition, we provide the results when the main task is classifying digits (MNIST) and the auxiliary task is classifying clothes (FashionMNIST), where sr is gray domain, t is color domain, m is classifying MNIST and a is classifying FashionMNIST. Figure 5(b) shows \hat{x}_{sr}^m , \hat{x}_t^m , \hat{x}_{sr}^a and \hat{x}_t^a . They are depicted with feature representations of patterns learned in their corresponding domains. For instance, \hat{x}_{sr}^m shows learned patterns of digits in the grayscale domain (MNIST), and \hat{x}_t^a shows learned patterns of clothes in the color domain (FashionMNIST). These results are admissible and expected due to their optimizing objectives and access of corresponding data. However, \hat{x}_t^m , shown in Figure 5(b), contains patterns of digits in the color domain, whose data are not accessed during training. These results show that TG-ZDA can learn representations of MNIST digits in color domain, in the manner of zero-shot, although it is never trained by images of digits from the target color domain.

Conclusion

ZDA problem is defined as training models where the target test data cannot be accessed in training phase. We have proposed a novel framework called TG-ZDA which employs a multi-branch DNN to solve this problem. The proposed TG-ZDA disentangles ZDA hypotheses to three functions. Each function is realized by a branch of a segment in TG-ZDA. Branches in the segments are recombined according to tasks. TG-ZDA learns domain specific features and shareability to overcome the absence of target data. Experimental results demonstrate that our proposed TG-ZDA outperforms state-of-the-art methods in benchmark ZDA tasks, validating the effectiveness of TG-ZDA.

References

- Arjovsky, M.; Bottou, L.; Gulrajani, I.; and Lopez-Paz, D. 2020. Invariant Risk Minimization. arXiv:1907.02893.
- Bau, D.; Zhu, J.-Y.; Strobelt, H.; Lapedriza, A.; Zhou, B.; and Torralba, A. 2020. Understanding the role of individual units in a deep neural network. *Proceedings of the National Academy of Sciences*, 117(48): 30071–30078.
- Borgwardt, K. M.; Gretton, A.; Rasch, M. J.; Kriegel, H.-P.; Schölkopf, B.; and Smola, A. J. 2006. Integrating structured biological data by kernel maximum mean discrepancy. *Bioinformatics*, 22(14): e49–e57.
- Bousmalis, K.; Silberman, N.; Dohan, D.; Erhan, D.; and Krishnan, D. 2017. Unsupervised pixel-level domain adaptation with generative adversarial networks. In *Proceedings of the IEEE Conference on Computer Vision and Pattern Recognition (CVPR)*, 3722–3731.
- Chattopadhyay, P.; Balaji, Y.; and Hoffman, J. 2020. Learning to Balance Specificity and Invariance for In and Out of Domain Generalization. In Vedaldi, A.; Bischof, H.; Brox, T.; and Frahm, J.-M., eds., *Proceedings of the European Conference on Computer Vision (ECCV)*, 301–318.
- Chen, C.; Fu, Z.; Chen, Z.; Jin, S.; Cheng, Z.; Jin, X.; and Hua, X. 2020. HoMM: Higher-order Moment Matching for Unsupervised Domain Adaptation. In *Proceedings of the AAAI Conference on Artificial Intelligence*, 3422–3429.
- Cohen, G.; Afshar, S.; Tapson, J.; and van Schaik, A. 2017. EMNIST: Extending MNIST to handwritten letters. In *2017 International Joint Conference on Neural Networks (IJCNN)*, 2921–2926.
- Creager, E.; Jacobsen, J.-H.; and Zemel, R. 2021. Environment Inference for Invariant Learning. In *International Conference on Machine Learning*.
- Fowlkes, E. B.; and Mallows, C. L. 1983. A Method for Comparing Two Hierarchical Clusterings. *Journal of the American Statistical Association*, 78(383): 553–569.
- Ganin, Y.; Ustinova, E.; Ajakan, H.; Germain, P.; Larochelle, H.; Laviolette, F.; Marchand, M.; and Lempitsky, V. 2016. Domain-adversarial training of neural networks. *The Journal of Machine Learning Research*, 17(1): 2096–2030.
- Grother, P. 1970. NIST Special Database 19. NIST Handprinted Forms and Characters Database.
- Gulrajani, I.; and Lopez-Paz, D. 2020. In Search of Lost Domain Generalization. arXiv:2007.01434.
- Huang, S.-W.; Lin, C.-T.; Chen, S.-P.; Wu, Y.-Y.; Hsu, P.-H.; and Lai, S.-H. 2018. Auggan: Cross domain adaptation with gan-based data augmentation. In *Proceedings of the European Conference on Computer Vision (ECCV)*, 718–731.
- Huang, X.; and Belongie, S. J. 2017. Arbitrary Style Transfer in Real-Time with Adaptive Instance Normalization. *Proceedings of the IEEE International Conference on Computer Vision (ICCV)*, 1510–1519.
- Johansson, F. D.; Sontag, D.; and Ranganath, R. 2019. Support and invertibility in domain-invariant representations. In *The 22nd International Conference on Artificial Intelligence and Statistics*, 527–536.
- Kamath, P.; Tangella, A.; Sutherland, D.; and Srebro, N. 2021. Does Invariant Risk Minimization Capture Invariance? In *Proceedings of The 24th International Conference on Artificial Intelligence and Statistics*, 4069–4077.
- Kutbi, M.; Peng, K.-C.; and Wu, Z. 2021. Zero-shot Deep Domain Adaptation with Common Representation Learning. *IEEE Transactions on Pattern Analysis and Machine Intelligence*, 1–1.
- Lampinen, A. K.; and McClelland, J. L. 2020. Transforming task representations to perform novel tasks. *Proceedings of the National Academy of Sciences*, 117(52): 32970–32981.
- LeCun, Y.; Bengio, Y.; and Hinton, G. 2015. Deep Learning. *Nature*, 521(7553): 436–444.
- Lecun, Y.; Bottou, L.; Bengio, Y.; and Haffner, P. 1998. Gradient-based learning applied to document recognition. *Proceedings of the IEEE*, 86(11): 2278–2324.
- Lee, C.-Y.; Batra, T.; Baig, M. H.; and Ulbricht, D. 2019. Sliced Wasserstein Discrepancy for Unsupervised Domain Adaptation. In *Proceedings of the IEEE Conference on Computer Vision and Pattern Recognition (CVPR)*, 10277–10287.
- Li, B.; Wang, Y.; Zhang, S.; Li, D.; Keutzer, K.; Darrell, T.; and Zhao, H. 2021. Learning Invariant Representations and Risks for Semi-Supervised Domain Adaptation. In *Proceedings of the IEEE Conference on Computer Vision and Pattern Recognition (CVPR)*, 1104–1113.
- Liang, J.; Hu, D.; and Feng, J. 2020. Do We Really Need to Access the Source Data? Source Hypothesis Transfer for Unsupervised Domain Adaptation. In *International Conference on Machine Learning (ICML)*, 6028–6039.
- Liu, H.; Long, M.; Wang, J.; and Jordan, M. 2019a. Transferable Adversarial Training: A General Approach to Adapting Deep Classifiers. In *Proceedings of the 36th International Conference on Machine Learning*, 4013–4022.
- Liu, M.-Y.; and Tuzel, O. 2016. Coupled Generative Adversarial Networks. In *Advances in Neural Information Processing Systems*, 469–477.
- Liu, S.; Ozay, M.; Xu, H.; Lin, Y.; and Okatani, T. 2019b. A Generative Model of Underwater Images for Active Landmark Detection and Docking. *2019 IEEE/RSJ International Conference on Intelligent Robots and Systems (IROS)*, 8034–8039.
- Lloyd, S. 1982. Least squares quantization in PCM. *IEEE transactions on information theory*, 28(2): 129–137.
- Luo, Y.; Zheng, L.; Guan, T.; Yu, J.; and Yang, Y. 2019. Taking a Closer Look at Domain Shift: Category-Level Adversaries for Semantics Consistent Domain Adaptation. *Proceedings of the IEEE Conference on Computer Vision and Pattern Recognition (CVPR)*, 2502–2511.
- Motiiian, S.; Jones, Q.; Iranmanesh, S.; and Doretto, G. 2017. Few-shot adversarial domain adaptation. In *Advances in Neural Information Processing Systems (NeurIPS)*, 6670–6680.
- Müller, A. C.; and Guido, S. 2016. *Introduction to machine learning with Python: a guide for data scientists*. ” O’Reilly Media, Inc.”.

- Peng, K.-C.; Wu, Z.; and Ernst, J. 2018. Zero-Shot Deep Domain Adaptation. In Ferrari, V.; Hebert, M.; Sminchisescu, C.; and Weiss, Y., eds., *Proceedings of the European Conference on Computer Vision (ECCV)*, 793–810.
- Poggio, T.; Banburski, A.; and Liao, Q. 2020. Theoretical issues in deep networks. *Proceedings of the National Academy of Sciences*, 117(48): 30039–30045.
- Rosenfeld, E.; Ravikumar, P.; and Risteski, A. 2021. The Risks of Invariant Risk Minimization. arXiv:2010.05761.
- Saxe, A. M.; McClelland, J. L.; and Ganguli, S. 2019. A mathematical theory of semantic development in deep neural networks. *Proceedings of the National Academy of Sciences*, 116(23): 11537–11546.
- Sejnowski, T. J. 2020. The unreasonable effectiveness of deep learning in artificial intelligence. *Proceedings of the National Academy of Sciences*, 117(48): 30033–30038.
- Simonyan, K.; and Zisserman, A. 2015. Very Deep Convolutional Networks for Large-Scale Image Recognition. arXiv:1409.1556.
- Sun, B.; Feng, J.; and Saenko, K. 2015. Return of Frustratingly Easy Domain Adaptation. arXiv:1511.05547.
- Sun, B.; and Saenko, K. 2016. Deep coral: Correlation alignment for deep domain adaptation. In *Proceedings of the European Conference on Computer Vision (ECCV)*, 443–450.
- Tang, H.; and Jia, K. 2020. Discriminative Adversarial Domain Adaptation. In *Proceedings of the AAAI Conference on Artificial Intelligence*, 5940–5947.
- Tzeng, E.; Hoffman, J.; Saenko, K.; and Darrell, T. 2017. Adversarial discriminative domain adaptation. In *Proceedings of the IEEE Conference on Computer Vision and Pattern Recognition (CVPR)*, 7167–7176.
- Tzeng, E.; Hoffman, J.; Zhang, N.; Saenko, K.; and Darrell, T. 2014. Deep Domain Confusion: Maximizing for Domain Invariance. arXiv:1412.3474.
- van der Maaten, L.; and Hinton, G. 2008. Visualizing Data using t-SNE. *Journal of Machine Learning Research*, 9(86): 2579–2605.
- Wang, J.; Cheng, M.-M.; and Jiang, J. 2021. Domain Shift Preservation for Zero-Shot Domain Adaptation. *IEEE Transactions on Image Processing*, 30: 5505–5517.
- Wang, J.; and Jiang, J. 2019. Conditional Coupled Generative Adversarial Networks for Zero-Shot Domain Adaptation. 3374–3383.
- Wang, J.; and Jiang, J. 2020. Adversarial Learning for Zero-shot Domain Adaptation. In *Proceedings of the European Conference on Computer Vision (ECCV)*, 329–344.
- Wang, J.; and Jiang, J. 2021. Learning across Tasks for Zero-Shot Domain Adaptation from a Single Source Domain. *IEEE Transactions on Pattern Analysis and Machine Intelligence*.
- Wang, T.; Zhang, X.; Yuan, L.; and Feng, J. 2019. Few-Shot Adaptive Faster R-CNN. *Proceedings of the IEEE Conference on Computer Vision and Pattern Recognition (CVPR)*, 7166–7175.
- Xia, H.; and Ding, Z. 2020. HGNet: Hybrid Generative Network for Zero-Shot Domain Adaptation. In *Proceedings of the European Conference on Computer Vision (ECCV)*, 55–70.
- Xiao, H.; Rasul, K.; and Vollgraf, R. 2017. Fashion-MNIST: a Novel Image Dataset for Benchmarking Machine Learning Algorithms. arXiv:1708.07747.
- Xu, M.; Zhang, J.; Ni, B.; Li, T.; Wang, C.; Tian, Q.; and Zhang, W. 2019a. Adversarial Domain Adaptation with Domain Mixup. arXiv:1912.01805.
- Xu, X.; Zhou, X.; Venkatesan, R.; Swaminathan, G.; and Majumder, O. 2019b. d-SNE: Domain Adaptation Using Stochastic Neighborhood Embedding. In *Proceedings of the IEEE Conference on Computer Vision and Pattern Recognition (CVPR)*, 2492–2501.
- Zhang, Y.; Liu, T.; Long, M.; and Jordan, M. 2019. Bridging Theory and Algorithm for Domain Adaptation. In *International Conference on Machine Learning*, 7404–7413.
- Zhao, H.; Combes, R. T. D.; Zhang, K.; and Gordon, G. 2019. On Learning Invariant Representations for Domain Adaptation. In Chaudhuri, K.; and Salakhutdinov, R., eds., *Proceedings of the 36th International Conference on Machine Learning*, volume 97 of *Proceedings of Machine Learning Research*, 7523–7532.